DIRECT TIME DOMAIN ANALYSIS OF AN UWB PULSE DISTORTION BY CONVEX OBJECTS WITH THE SLOPE DIFFRACTION INCLUDED

P. Górniak, W. Bandurski, Poznań University of Technology

Abstract - **The paper deals with time domain (TD) modelling of diffraction of a signal, caused by 2D conducting convex objects for soft polarization case. Two models of the amplitude term of the time domain convex obstacle diffraction coefficient are proposed and compared. One model is derived using an analytical-numerical method and the other is obtained in a purely analytical way. Both methods use Uniform Geometrical Theory of Diffraction (UTD) formulated in the frequency domain (FD). The models are used to examine an Ultra Wide Band (UWB) pulse distortion. The accuracy and calculation complexity of both models are compared. The slope term of the convex obstacle diffraction coefficient is also considered, for the case when slope diffraction is not negligible. The UWB pulse distortion caused by overall convex obstacle diffraction is also analysed.**

1 INTRODUCTION

The UWB communication has received a great deal of attention in recent years [1-3]. The large bandwidth of UWB signals offers rapid increase in data transmission speed on the one hand, and greater accuracy of positioning and object detection on the other hand. However, this large bandwidth of UWB signals introduces some problems nonexistent or negligible in narrowband data transmission. The distortion of an UWB pulse is one such problem. Since the propagation loss is frequency dependent, the frequency spectrum of the transmitted UWB signal is significantly changed during propagation. This phenomenon has been discussed in a number of papers, e.g. [4-7].

Pulse distortion is mainly caused by scattering objects such as walls, edges and rounded surfaces [8, 19]. The propagation between scattering objects does not affect pulse shapes, but rather involves pulse delays [5-8]. An example of a scattering object is an obstacle with a rounded shape. Such a scattering object has its own frequency response and equivalent impulse response. In the case of UWB propagation, using the impulse response of a scattering object is more convenient for analysing the propagation of the transmitted UWB pulse. If the impulse response of the scattering object is known, the time domain characteristics of the distorted UWB pulse can be found through an operation of convolution. In particular, time domain results can give more insight in baseband data transmission, which is an option in an UWB communication system. It is also helpful in determining time delay parameters of the channel in such areas as synchronization, positioning and detection.

In principle, the impulse response of a convex object incorporates two terms corresponding to the phenomena of reflection and diffraction, respectively. At least one of these phenomena occurs for a given position of transmitter and receiver in a non-line-of-sight situation (NLOS).

In our paper we deal with one of these phenomena, i.e. with diffraction. The process of diffraction caused by a convex object determined in the time domain has some coverage in literature, e.g. in the paper of J. R. Wait and A. M. Conda [9]. Wait and Conda find the electric currents induced on a circular cylinder when it is excited by a temporal step-function plane wave. The currents are approximated in the frequency domain by an Airy integral. The approximate frequency domain result is valid when the radius of the cylinder is large compared to wavelength. Then the authors expand the FD expression into a power series and use an inverse Laplace transform to obtain an asymptotic series of inverse powers of time. In the second part of their paper, they discuss the

diffraction by a smooth surface when the source and observer are removed from the surface. They solve the special case of a cylinder, although they mention that these results can be easily generalized. Their solution is valid for observation points near the shadow boundary. More examples, including the transient scattering by a circular cylinder, are discussed in [13].

Another important issue is the transition zone diffraction, where the slope diffraction plays a significant role. Transition zone diffraction occurs when the scattering objects are relatively close to the shadow boundaries of the scenario. This problem has also been discussed in the literature, e.g. by J. B. Andersen [14], who developed a FD model concerning transition zone diffraction on screen edges. R. Qiu in [8] presents a time domain model of propagation of EM wave signal over a row of buildings of the same height. P. H. Pathak in [16] derives the time domain version of slope diffraction on curved wedge. This is an extension of paper [15], which discusses time domain amplitude diffraction on a curved wedge. G. Koutitas in [17] discusses the FD model of the transition zone diffraction over convex obstacles, where slope diffraction is a very significant factor

In our paper we derive the time domain version of the model of two cascaded convex obstacles shadowing a transmitter and a receiver for soft polarization case. We find the time domain convex object diffraction coefficient which comprises both the amplitude term and the slope term. We obtain it in a different way from that in [9]. We use the frequency domain Uniform Geometrical Theory of Diffraction, presented in [10, 11]. A similar method concerning the amplitude term of convex object diffraction coefficient was used in [12] and [13], where FD-UTD for convex objects was also a starting point. In [12] the authors use the inverse Laplace transform in order to find the time domain convex obstacle diffraction coefficient, while in [13] the one-sided inverse Fourier transform is used. In our paper we use both inverse Laplace transform and one-sided inverse Fourier transform as well as some numerical approximations. First we focus on the amplitude term of the time domain convex obstacle diffraction coefficient. We obtain the amplitude term in two ways, applying first an

analytical-numerical approach and next a purely analytical approach. Then we find the slope term of the time domain convex object diffraction coefficient. We use the derived amplitude and slope term of the time domain convex obstacle diffraction coefficient to examine the impact of convex obstacles on the shape and time characteristics of a propagating UWB pulse.

The paper is organised as follows. In Section 2 we describe the model of a given convex obstacle and its parameters. Section 3 presents the transformation of the FD diffraction coefficient of a convex object into the time domain. We present two methods for performing the transformation. The first is an analytical-numerical method involving Laplace transform and the algorithm of rational function approximation, called vector fitting. The second is a purely analytical method involving inverse Laplace transform and one-sided inverse Fourier transform. We compare the two methods in terms of their correctness. In Section 4 we show how to obtain the time domain version of the slope term of the diffraction coefficient of a convex obstacle. Section 5 gives an example of the slope diffraction application for the case of two convex obstacles diffraction. Finally, the summary and conclusions are presented in Section 6.

2. DEFINITION OF THE BARE HILL CHANNEL TRANSFER FUNCTION

One example of convex object is a 2D bare hill. It can be modeled as a part of a circle, as
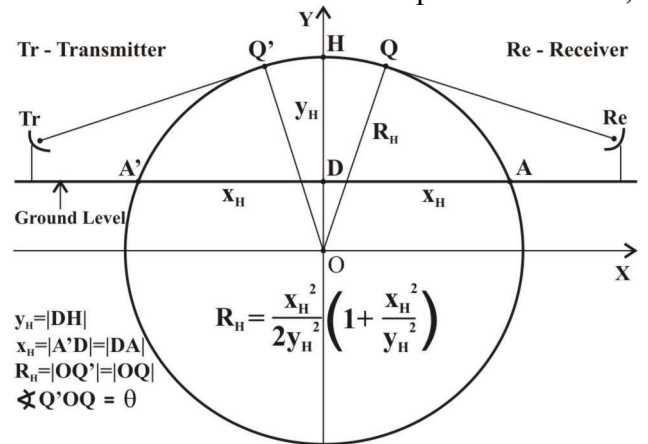

Fig. 1. Model of a bare hill.

shown in Fig. 1. This model was proposed by H. Bertoni, [21]. The arc of the circle is limited by a chord of length $2x_H$. The height of the hill is equal

to y_H. Knowing x_H and y_H, we can calculate the radius of the hill, R_H. We assume that the transmitted pulse approaches the receiver along one dominant ray, which is a creeping ray. The ray becomes "attached" the hill at attachment point Q'. Then it travels along the arc of the hill. The ray leaves the arc of the hill tangentially at the shedding point Q. Therefore the transmitted pulse experiences diffraction on the convex obstacle. The distortion of the pulse is determined by the transfer function over the distance Q'Q. The distortion caused by propagation in the air can be neglected.

In this paper, in order to find the time domain convex obstacle diffraction coefficient we use the frequency domain Uniform Geometrical Theory of Diffraction (UTD) [10, 11]. The exact UTD expression for the frequency domain diffraction coefficient for soft polarization of one convex obstacle is given by (1) [18, 20], and the parameters of the model are indicated in Fig. 1 [21].

$$H_A(\omega) = -m\sqrt{\frac{2}{\beta}}e^{-j\frac{\pi}{4}}\left(\frac{-F(X_d)}{2\xi_d\sqrt{\pi}} + p^*(\xi_d)\right) \tag{1}$$

The diffraction coefficient (transfer function $H_A(\omega)$) given by (1) does not include the delay terms or spreading factor. The parameters used in (1) are as follows:

$$m(\omega, R) = \left(\frac{\omega R}{2c}\right)^{\frac{1}{3}},$$

$$\xi_d(\omega, \theta, R) = m(\omega, R) \cdot \theta,$$

$$X_d = \frac{\omega L \xi_d^2}{2cm^2} = \frac{\omega L \theta^2}{2c},$$

where $\beta = \omega/c$, c is the speed of electromagnetic wave propagation in free space and L is the distance parameter, which can be defined in the following form (using notation shown in Fig. 1):

$$L = \frac{|TrQ| \cdot |Q\,\mathrm{Re}|}{|TrQ| + |Q\,\mathrm{Re}|},$$

$F(X)$ is the transition function and $p^*(x)$ is the special Fock scattering function, determined by the following integrals:

$$F(x) = 2j\sqrt{x}e^{jx}\int_{\sqrt{x}}^{\infty}e^{-ju^2}du, \tag{2}$$

$$p^*(x) = \frac{1}{\sqrt{\pi}}\int_{-\infty}^{\infty}\frac{V(\tau)e^{-jx\tau}}{W_2(\tau)}d\tau, \tag{3}$$

where:

$$V(\tau) = \sqrt{\pi}Ai(\tau), \qquad W_2(\tau) = \frac{1}{\sqrt{\pi}}\int_{\infty e^{j2\pi/3}}^{\infty}e^{\frac{-z^3}{3}}e^{\tau z}dz,$$

and

$$Ai(\tau) = \int_{0}^{\infty}\cos\left(\tau z + \frac{z^3}{3}\right)dz.$$

3. IMPULSE RESPONSE OF A BARE HILL

For a bare hill, the impulse response is equivalent to the time domain diffraction coefficient of the hill model described in the previous section. It is a TD-UTD formulation which incorporates all properties and assumptions of the FD-UTD theory, formulated for the diffraction on smooth convex surfaces. The impulse response of a bare hill is obtained in two ways, in an analytical-numerical way and in a purely analytical way.

A. ANALYTICAL-NUMERICAL METHOD

In order to transform (1) into the time domain, we split it into two components:

$$H_1(\omega) = m\sqrt{\frac{2}{\beta}}e^{-j\frac{\pi}{4}}\frac{F(X_d)}{2\xi_d\sqrt{\pi}}, \tag{4}$$

$$H_2(\omega) = -m\sqrt{\frac{2}{\beta}}e^{-j\frac{\pi}{4}}p^*(\xi_d). \tag{5}$$

The transition function $F(X)$ in (4) can be expressed as a complementary error function:

$$erfc(x) = \frac{2}{\sqrt{x}}\int_{x}^{\infty}e^{-t^2}dt \tag{6}$$

Comparing (2) and (6), we can define the transition function F(X) in the following way:

$$F(X_d) = e^{j\frac{\pi}{4}} \sqrt{\pi X_d} \, e^{jX_d} \, erfc\left(\sqrt{jX_d}\right) \qquad (7)$$

After substituting jω=p and performing some manipulations we have:

$$H_1(p) = \frac{1}{\sqrt{\pi}} \frac{R_H}{\sqrt{2D}} \sqrt{\pi X} \, e^{p\frac{X}{c}} \, erfc\left(\sqrt{\frac{pX}{c}}\right), \qquad (8)$$

where:

$$X = \frac{L_d \theta^2}{2}. \qquad (9)$$

From the Laplace transform table we have:

$$\sqrt{\pi X} \, e^{p\frac{X}{c}} \, erfc\left(\sqrt{\frac{pX}{c}}\right) \leftrightarrow \frac{X}{\sqrt{\pi c t}\left(t + \frac{X}{c}\right)}. \qquad (10)$$

Taking into account relationships (10) and (8), we can present inverse Laplace transform of $H_1(p)$ by the following formula [8]:

$$h_1(t) = L^{-1}\left[H_1(p)\right] = \frac{R_H X}{\pi D \sqrt{2ct}\left(t + \frac{X}{c}\right)} \qquad (11)$$

Transfer function $H_2(\omega)$ cannot be easily transformed to the time domain in an analytical way because of the Fock scattering function incorporated in it. We will consider the analytical way later. In this section we propose to approximate $H_2(\omega)$ with a rational function. To do this, we use a new and very effective method called vector fitting, worked out by B. Gustavsen [22]. This method describes a way of fitting the measured or calculated values of a signal Fourier spectrum to the approximating function of the following form:

$$f(p) = \sum_{n=1}^{N} \frac{c_n}{p - a_n} + d + ph \qquad (12)$$

Vector fitting allows us to find, in an iterative way, such values of residues c_n, d, h and poles a_n, that f(p) is very well fitted to measured or calculated data. The code of the algorithm is given in Matlab language, [23]. The algorithm needs on its input the initial values of poles a_n. In order to approximate smooth functions, the values of these poles should be the values of frequencies distributed linearly or logarithmically over the whole given frequency band.

In order to use the vector fitting algorithm, we calculated $H_2(\omega)$ numerically for the frequencies up to 20 GHz, with the parameters of the hill $R_H=2500m$ and $\theta=0.08m$. Then by running the vector fitting program we obtained the values of residues and poles of the function f(p) for N=7. The results of the approximation of the transfer function $H_2(\omega)$ for given parameters are shown in Fig. 2.
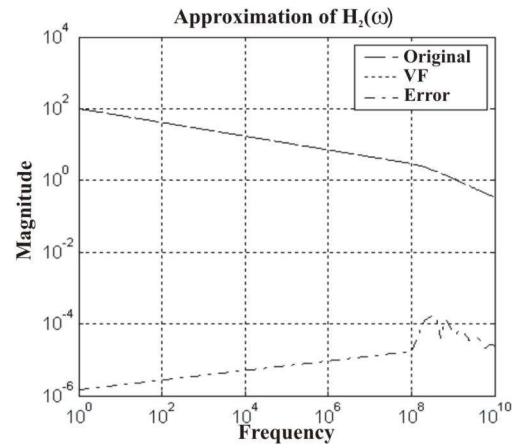

Fig.2. Amplitude characteristic of $H_2(\omega)$, its approximation and the error of approximation.

We see that the approximating function is very well fitted to the approximated function and the maximum relative error of approximation of the amplitude of $H_2(\omega)$ is slightly bigger than 10^{-4}.

The inverse Laplace transform of (12) is as follows:

$$h_2(t) = \sum_{n=1}^{N} c_n e^{a_n t} + d\delta(t) + h\delta'(t). \qquad (13)$$

The final form of the impulse response of the hill is the sum of expressions (11) and (13):

$$h_A(t) = h_1(t) + h_2(t) \qquad (14)$$

It is worth mentioning that vector fitting is not suitable for approximation of $H_1(\omega)$ and even with 40 poles (12) does not fit $H_1(\omega)$ well. The reason of this is that the imaginary part of $H_1(\omega)$ cannot be easily approximated by a hyperbolic function.

B. PURELY ANALYTICAL METHOD

In this section we present the purely analytical method of obtaining the convex obstacle diffraction coefficient. From now on, we will call this method the analytical method.

Formula (1) cannot be directly transformed into the time domain in an analytical way. It must be first presented in the following form [10]:

$$H_A(\omega) = -m\sqrt{\frac{2}{\beta}}\left(\frac{e^{-j\pi/4} \cdot (1 - F(X_d))}{2\xi_d\sqrt{\pi}} + P_s(\xi_d)\right), \qquad (15)$$

where $P_s(\xi_d)$ is the Pekeris caret function, which is in the following relationship with the Fock scattering function

$$P_s(x) = p^*(x) \cdot e^{-j\pi/4} - \frac{e^{-j\pi/4}}{2x\sqrt{\pi}}. \qquad (16)$$

Now $H_A(\omega)$ contains two components:

$$H_A(\omega) = H_{A1}(\omega) + H_{A2}(\omega)$$

where:

$$H_{A1}(\omega) = H_{A11}(\omega) + H_{A12}(\omega) \qquad (17)$$

$$H_{A11}(\omega) = -m\sqrt{\frac{2}{k}}e^{-j\pi/4}\frac{1}{2\xi_d\sqrt{\pi}}, \qquad (18)$$

$$H_{A12}(\omega) = m\sqrt{\frac{2}{k}}e^{-j\pi/4}\frac{F(X_d)}{2\xi_d\sqrt{\pi}}, \qquad (19)$$

and

$$H_{A2}(\omega) = -m\sqrt{\frac{2}{k}}P_s(\xi_d). \qquad (20)$$

The above components have different forms from those used in Section 3A. We substituted the Pekeris caret function to (1), because thanks to it the second component of $H_A(\omega)$ (20) can be approximated by a fast converging series. It could not be done in the previous section, and $H_2(\omega)$ was approximated numerically. Now $H_A(\omega)$ given by (15) can be easily transformed to the time domain. First we approximate (20). It can be approximated by two different series, depending on the value of the argument of the Pekeris caret function. The first one (for bigger values of ξ_d) is the series expansion given by Keller [10]:

$$H_{A2}(\omega) \approx \sum_{n=0}^{N} D_n \cdot e^{-\alpha_n\theta}, \qquad (21)$$

where:

$$D_n = \sqrt{\frac{1}{2\pi k}} \cdot \frac{m}{[Ai'(q_n)]^2} \cdot e^{-j\pi/12}, \qquad (22)$$

$$\alpha_n = -q_n m\theta \cdot e^{j\pi/6}, \qquad (23)$$

q_n are zeros of the Airy function and $Ai'(q_n)$ is the value of the derivative of the Airy function for q_n. The values of q_n and $Ai'(q_n)$ can be found in [10].

The second approximating series is related to smaller values of ξ_d (down to 0), which correspond to the values of field in transition zones. In this situation we propose to use the approximation of the Fock scattering function for the case of soft polarization for small ξ_d [24]:

$$p^*(\xi_d) \approx e^{j\pi/6}\sum_{n=1}^{N}\frac{\rho_n}{n!} \cdot j^{n/3} \cdot \xi_d{}^n, \qquad (24)$$

The values of coefficients ρ_n can be found in [13, 24].

Now the question is what is the best threshold value of ξ_d, for which (20) can be approximated with sufficient accuracy (by this we mean that the relative deviation is less than or equal to 3% and at the same time the number of series terms is as

small as possible). The calculations which we conducted have shown that this threshold value is about $\xi_{dT} = 0.35$. The closer the value of ξ_d is to the threshold, the bigger number of series terms is needed for appropriate approximation of (19). The maximum required number of terms in (21) and (24) equals 12 and 5, respectively. The more the value of ξ_d differs (in either way) from the threshold value $\xi_{dT} = 0.35$, the fewer term in (21) and (24) are needed, reaching at the limit only one term. When the threshold value of ξ_{dT} is moved from 0.35 towards either side, the number of needed terms in (21) or (24) in the threshold vicinity rapidly increases.

For $\xi_d > 0.35$ (20) is approximated by Keller's series. First we must transform Keller's series to the time domain. In order to do this, we substitute (22) and (23) to (21). After rearranging, (21) takes the following form:

$$H_{A2}(\omega) \approx H_{A2>}(\omega) = \sum_{n=0}^{N} A_n \cdot \omega^{-1/6} \cdot e^{-\gamma_n \omega^{1/3}\theta}, \qquad (25)$$

where:

$$A_n = \left(\frac{R}{2c}\right)^{1/3} \cdot j^{-1/6} \cdot \sqrt{\frac{c}{2\pi}} \cdot \frac{1}{[Ai'(q_n)]^2}, \qquad (26)$$

$$\gamma_n = -q_n \left(j \frac{R}{2c}\right)^{1/3}. \qquad (27)$$

In order to approximate (20) for $\xi_d \leq 0.35$ we substitute (24) to (16), which results in the following series expansion:

$$H_{A2}(\omega) \approx H_{A2<}(\omega) = m\sqrt{\frac{2c}{\omega}} e^{-j\pi/4} \cdot \\ \cdot \left(\frac{1}{2\xi\sqrt{\pi}} - e^{j\pi/6} \sum_{n=0}^{N} \frac{\rho_n}{n!} j^{n/3} \xi_d^{\ n}\right). \qquad (28)$$

Finally, the approximation of $H_{A2}(\omega)$ can be written in the following form:

$$H_{A2}(\omega) \approx \begin{cases} H_{A2>}(\omega) & \xi_d > 0.35 \\ H_{A2<}(\omega) & \xi_d \leq 0.35 \end{cases} \qquad (29)$$

After approximating (20) we can transform (15) into the time domain using the inverse Laplace transform (as in the case of $H_1(\omega)$) and the one-sided inverse Fourier transform, where time t_c may be a complex number [11,13]:

$$\overset{+}{f}(t_c) = \frac{1}{\pi} \int_0^\infty F(\omega) e^{j\omega t_c} d\omega. \qquad (30)$$

Then the corresponding real time function can be found using the expression:

$$f(t) = \text{Re}\left[\overset{+}{f}(t_c)\right]. \qquad (31)$$

In order to apply (30) to (18), (19), (25) and (28), we must find the following integrals:

$$I_1(t) = \int_0^\infty \omega^a e^{-\gamma\omega^{1/3}\theta} e^{j\omega t} d\omega, \qquad (32)$$

$$I_2(t) = \int_0^\infty \omega^a e^{j\omega t} d\omega. \qquad (33)$$

Integral (32) is calculated using Taylor's series expansion of the factor $e^{j\omega t}$ around $\omega=0$. After integrating, $I_1(t)$ can be approximated by the following series:

$$I_1(t) \approx \frac{3}{(\gamma\theta)^{3(1+a)}} \sum_{n=0}^{N} \frac{j^n}{n!} \Gamma[3(n+1+a)]\left(\frac{t}{(\gamma\theta)^3}\right)^n. \qquad (34)$$

For very small values of $\left(\frac{t}{(\gamma\theta)^3}\right)$, $I_1(t)$ converges for small N.

After integration, (33) has the form:

$$I_2(t) = \left(\frac{-1}{jt}\right)^{a+1} \Gamma(a+1), \qquad (35)$$

where $a>-2$.

Now we can give the time domain equivalents of expressions (18), (19), (25) and (28):

$$\overset{+}{h}_{A11}(t) = -\frac{1}{\pi}\sqrt{\frac{c}{2\pi}} \frac{e^{-j\pi/4}}{\theta}\left(\frac{-1}{jt}\right)^{1/2}\Gamma\left(\frac{1}{2}\right). \qquad (36)$$

$$h_{A12}(t) = \frac{L\theta}{2\pi\sqrt{2ct}\left(t + \dfrac{X}{c}\right)}, \tag{37}$$

$$h_{A2>}^{+}(t) = \frac{1}{\pi}\sum_{n=0}^{N} A_n \frac{3}{(\gamma_n\theta)^{\frac{5}{2}}}\sum_{m=0}^{M}\frac{j^m}{m!}\Gamma\left(3m+\frac{5}{2}\right)\cdot\left[\frac{t}{(\gamma_n\theta)^3}\right], \tag{38}$$

$$h_{A2<}^{+}(t) \approx \frac{1}{\pi}\sum_{n=0}^{N} B_n\theta^n\left(\frac{-1}{jt}\right)^{\frac{n}{3}+\frac{5}{6}}\Gamma\left(\frac{n}{3}+\frac{5}{6}\right) + \frac{1}{\pi}\sqrt{\frac{c}{2\pi}}\frac{e^{-j\pi/4}}{\theta}\left(\frac{-1}{jt}\right)^{1/2}\Gamma\left(\frac{1}{2}\right). \tag{39}$$

where:

$$B_n = (2c)^{\frac{1}{6}}R^{\frac{1}{3}}\frac{\rho_n}{n!}\left(\frac{R}{2c}\right)^{\frac{n}{3}}j^{\frac{n}{3}-\frac{1}{6}} \tag{40}$$

The whole impulse response transformed from $H_A(\omega)$ has the form:

$$h_A(t) \approx \begin{cases} h_{A12}(t) + \text{Re}\left\{\overset{+}{h}_{A11}(t) + \overset{+}{h}_{A2<}(t)\right\} & \bigwedge\limits_{f\in B}\xi_d(f)\le 0.35 \\ h_{A12}(t) + \text{Re}\left\{\overset{+}{h}_{A11}(t) + \overset{+}{h}_{A2>}(t)\right\} & \bigwedge\limits_{f\in B}\xi_d(f)> 0.35 \end{cases}, \tag{41}$$

where B is the frequency band of the incident signal.

C. COMPARISON OF THE TWO METODS.

In this section we examine the accuracy of the results presented in sections 3A and 3B. In order to verify the accuracy of formulas (14) and (41) we examine the distortion of an UWB pulse caused by a single convex obstacle. It is done through the operation of convolution of the incident UWB pulse p(t) and (14) or (41). The pulse p(t) has two parameters, a and t_c, which are the width of the pulse and the middle argument of the pulse, respectively.

$$p(t) = \left[1 - 4\pi\left(\frac{t-t_c}{a}\right)^2\right]e^{-2\pi\left(\frac{t-t_c}{a}\right)^2} \tag{42}$$

The results of the convolution are compared with the results of frequency domain calculations obtained using IFFT (Fig. 3.) The parameters of

the convex object are the same as in Section 3A. Fig.3 shows the distorted pulse and the normalized transmitted pulse with its parameters set to the following values: a = 3ns, t_c = 1ns.
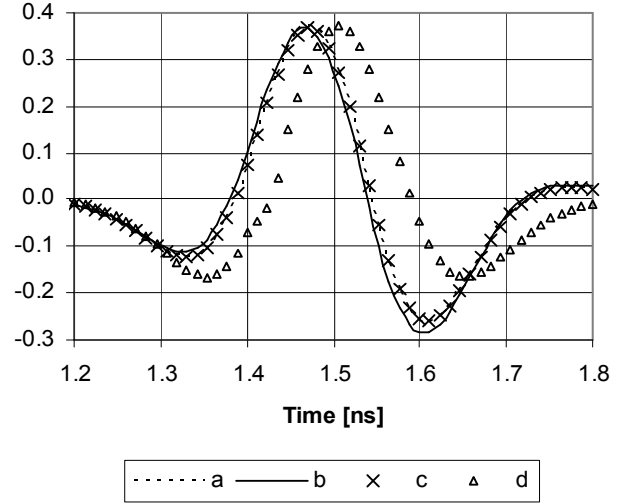
UWB pulse distortion (Amplitude diffraction)

Fig 3. Comparison of the incident UWB pulse and the distorted pulse calculated using the analytical-numerical method and analytical method: a – distorted pulse calculated using IFFT, b – distorted pulse calculated in time domain using the analytical-numerical method, c – distorted pulse calculated in the time domain using the analytical method, d – incident UWB pulse normalized to the amplitude of the distorted pulse.

We see that the accuracy of the results obtained by both methods is similar and very good (formula (41) is slightly more accurate). In the case of analytical-numerical method, 7 poles of the function f(p) approximating $H_1(\omega)$ are sufficient to achieve such accuracy. In the case of analytical method, the same results are achieved for the first 12 terms of (25) and for the first 5 terms of (28).

However, this method is not applicable in all circumstances. The conducted calculations have shown that formula (41) gives a very good agreement with the results of the calculations obtained using IFFT when $\left(\dfrac{t}{(\gamma\theta)^3}\right)<$ 0.00725. We shall call this condition (a). Then only 3 terms of expression (34) are required to make it convergent. If condition (a) is not fulfilled, formula (41) is still valid and gives very good results when $\xi_d\le0.35$ or equivalently when $t<10^{-6}$s, upper frequency of transmitted signals is less than or equal to 20GHz

and $R^{1/3}\theta < 0.11 m^{1/3}$rad. In other cases the method is not applicable because of weak convergence of (34).

Summering up, analytical method provides the closed form of the impulse response – (41), while formula (14) is not a generalized solution. It is related to a particular example of a convex obstacle; on the other hand, it does not have the limitations which occur in the analytical method.

4. SLOPE TERM OF THE FREQUENCY DOMAIN CONVEX OBSTACLE DIFFRACTION COEFFICIENT

When it comes to finding the diffraction caused by two cascaded convex objects, so that one convex object is in the transition zone of the previous one, slope diffraction is the factor to be determined. In the described situation slope diffraction plays a significant role in field distribution.

A. FREQUENCY DOMAIN FORMULATION

The slope term of the diffraction coefficient is defined by the following equation [14,17]:

$$H_s(\omega,s) = \frac{\partial H_A(\theta)}{s\partial\theta} = \frac{1}{s}\left(\frac{\partial H_{A1}(\theta)}{\partial\theta} + \frac{\partial H_{A2}(\theta)}{\partial\theta}\right), \quad (43)$$

where s is the distance from the point where the creeping ray leaves the convex obstacle to the point of observation. Taking into consideration the amplitude term and slope term of the convex object diffraction coefficient, the frequency response of the channel has the following form:

$$[H_s(\omega,s) + H_A(\omega)]A(s)e^{-jk(\theta R+s)}, \quad (44)$$

where the input of the channel is at point Q' in Fig. 1 and the output of the channel is at the point of observation in the shadow zone.

Performing the differentiation in (43), we obtain:

$$H_{S1}(\omega,s) = \frac{\partial H_{A1}(\theta)}{s\partial\theta} =$$
$$= H_{S11}(\omega,s) + H_{S12}(\omega,s) + H_{S13}(\omega,s) =$$
$$= -\sqrt{\frac{2c}{\omega}}e^{-j\pi/4}\frac{j\omega L}{2c\sqrt{\pi}s} + \sqrt{\frac{2c}{\omega}}e^{-j\pi/4}\frac{LF(X_d)}{2c\sqrt{\pi}s} +$$
$$+ \sqrt{\frac{2c}{\omega}}e^{-j\pi/4}\frac{1}{2s\sqrt{\pi}\theta^2}. \quad (45)$$

Using approximations of $H_{A2}(\omega,\theta)$ given by (25) and (28), after differentiation we obtain:

$$H_{S2}(\omega,s) = \frac{\partial H_{A2}(\theta)}{s\partial\theta} \approx \begin{cases} H_{S2<}(\omega,s) & \xi \le 0.35 \\ H_{S2>}(\omega,s) & \xi > 0.35 \end{cases} =$$

$$= \begin{cases} -\sqrt{\frac{2c}{\omega}}e^{-j\pi/4}\frac{1}{2s\sqrt{\pi}\theta^2} - \\ \quad -\sum_{n=0}^{N}\frac{n}{s}B_n\theta^{n-1}\omega^{\frac{n}{3}-\frac{1}{6}} & \xi \le 0.35 \\ -\sum_{n=0}^{N}\frac{A_n}{s}\gamma_n\omega^{\frac{1}{6}}e^{-\gamma_n\omega^{1/3}\theta} & \xi > 0.35 \end{cases} \quad (46)$$

B. TIME DOMAIN FORMULATION

To obtain the time domain version of (45) and (46), we use the analytical approach. Following the same steps as in Section 3B, we can write the time domain versions of expressions (45) and (46) in the form:

$$\overset{+}{h}_{S11}(t,s) = \frac{-1}{\pi}\sqrt{\frac{1}{2c\pi}}\frac{Le^{j\pi/4}}{s}\left(\frac{-1}{jt}\right)^{3/2}\Gamma\left(\frac{3}{2}\right) \quad (47)$$

$$h_{S12}(t,s) = \frac{\partial}{\partial t}\left(\frac{L^2\theta^2}{s2c\pi\sqrt{2ct}\left(t+\frac{X}{c}\right)}\right), \quad (48)$$

$$\overset{+}{h}_{S13}(t,s) = \frac{1}{\pi}\sqrt{\frac{c}{2\pi}}\frac{e^{-j\pi/4}}{s\theta^2}\left(\frac{-1}{jt}\right)^{1/2}\Gamma\left(\frac{1}{2}\right), \quad (49)$$

$$\overset{+}{h}_{S2<}(t,s) \approx \frac{1}{\pi}\sum_{n=0}^{N}\frac{nB_n}{s}\theta^{n-1}\left(\frac{-1}{jt}\right)^{\frac{n}{3}+\frac{5}{6}}\Gamma\left(\frac{n}{3}+\frac{5}{6}\right) -$$
$$\frac{1}{\pi}\sqrt{\frac{c}{2\pi}}\frac{e^{-j\pi/4}}{s\theta^2}\left(\frac{-1}{jt}\right)^{1/2}\Gamma\left(\frac{1}{2}\right), \quad (50)$$

$$\overset{+}{h}_{S2>}(t) = \frac{-1}{\pi}\sum_{n=0}^{N}\frac{A_n}{s}\frac{3}{(\gamma_n\theta)^{\frac{5}{2}}}\sum_{m=0}^{M}\frac{j^m}{m!}\Gamma\left(3m+\frac{7}{2}\right)\left[\frac{t}{(\gamma\theta)^3}\right]^m. \quad (51)$$

$$h_S(t,s) \approx \begin{cases} h_{S12}(t,s) + \\ \text{Re}\left\{ \sum_{n=1,3} \overset{+}{h}_{S1n}(t,s) + \overset{+}{h}_{s2<}(t,s) \right\} & \underset{f \in B}{\wedge} \xi_d(f) \le 0.35 \\ h_{S12}(t,s) + \\ \text{Re}\left\{ \sum_{n=1,3} \overset{+}{h}_{S1n}(t,s) + \overset{+}{h}_{s2>}(t,s) \right\} & \underset{f \in B}{\wedge} \xi_d(f) > 0.35 \end{cases} \quad (52)$$

5. MODEL OF THE CHANNEL WITH TWO CONVEX OBJECTS SHADOWING TRANSMITTER AND RECEIVER

The considered channel model is shown in Fig. 4. We assume that the slope of the field is zero when the field originates from the transmitter. We further assume that the receiver is in the far zone, so the slope of the field originating from the second obstacle equals zero. Then the field at the receiver is defined in the frequency domain by (53) (the time delay of the signal over the distance $\theta_{1/2}R_{1/2}$ is not included):

$$E_{Re} = \left(E_2 H_A(L_{A12Re}, R_2, \theta_2) + \frac{\partial E_2}{\partial n} D(L_{S12Re}, R_2, \theta_2) \right) \quad (53)$$
$$\cdot A_2(s) \cdot e^{-jl|2'Re|},$$

where:

$$E_2 = E_1 H_A(L_{ATr12}, R_1, \theta_1) A_1(s) e^{-jks_{12}}, \quad (54)$$
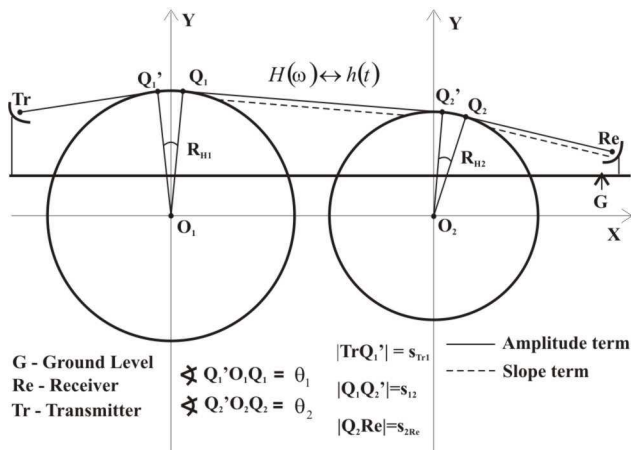

Fig. 4. Channel model containing two convex objects between transmitter and receiver.

$$\frac{\partial E_2}{\partial n} = E_1 H_s(L_{sTe12}, R_1, \theta_1, s_{12}) A_1(s) e^{-jks_{12}}, \quad (55)$$

$$D(L_{S12Re}, R_2, \theta_2) = \frac{s_{2Re} H_s(L_{sTe12}, R_1, \theta_1, s_{2Re})}{jk}. \quad (56)$$

E_1 is the value of the field at point 1, where the creeping ray hits the first convex object, L_{A12Re}, L_{S12Re} are the distance parameters ensuring the continuity of the amplitude term and slope term of the field about the shadow boundary after the second convex object, and L_{ATr12}, L_{STr12} are the distance parameters ensuring the continuity of the amplitude term and slope term of the field about the shadow boundary after the first convex object.

$$L_{ATr12} = L_{STr12} = \frac{s_{Tr1} s_{12}}{s_{Tr1} + s_{12}}. \quad (57)$$

The distance parameters L_{A12Re} and L_{S12Re} are generally frequency dependent [17]. However for some position of transmitting antenna with respect to convex obstacles and for higher frequencies (over 1GHz), L_{A12Re} and L_{S12Re} are approximately constant with very small imaginary part so they may be treated as real constants. The responses of the obstacles for the baseband UWB impulse (42) for frequency dependent or constant (frequency independent) L_{A12Re} and L_{S12Re} practically do not differ (the relative error does not exceed 1%). The above considerations are valid for the cases when s_{Tr1}, s_{12}, s_{2Re} are comparable with or larger than the radius of the first obstacle and additionally the angle θ_1 is sufficiently small. The smaller the radius of the first obstacle the greater the ratios R_1 / s_{Tr1}, R_1 / s_{12} and R_1 / s_{2Re} must be.

Other justification results from following observation: the smaller the values of the R_1^2 / L_{ATr12}^3 and θ_1 the closer the distance parameters L_{A12Re} and L_{S12Re} to a complex constant, which imaginary part tends to zero for higher frequencies. The numerical simulations conducted by us showed, that for example when $R_1 = 0.25$m and $s_{Tr1} = s_{12} = s_{2Re} = 2$m, the value of θ_1 can not be larger than 0.11 (for larger values of θ_1 the error resulting from treating the L_{A12Re} and L_{S12Re} as real constants is higher). The scenario related to the data $\theta_1 = 0.11$, $R_1 = 0.25$m and $s_{Tr1} = s_{12} = s_{2Re} = 2$m occurs when transmitting antenna and the first obstacle are collinear as well as the difference between the heights of the first and second obstacle is 0.22m.

Other scenario, related to the same data occurs when the obstacles are collinear and the difference between the transmitting antenna and the obstacles is 0.22m. For bigger obstacles when for example R_1=200m and for distances s_{Tr1}=400m, s_{12}=s_{2Re}=150m, the value of θ_1 can not exceed 0.2. With the assumptions given above, using the formulation derived in Section 3B and 4B , we obtain the time domain formulation of (53) in the form:

$$E_{Re}(t) = \left(E_2(t) * h_A(t, L_{A12Re}, R_2, \theta_2) + \frac{\partial E_2(t)}{\partial n} * d(t, L_{s12Re}, R_2, \theta_2) \right) A_2(s) * \delta\left(t - \frac{s_{2Re}}{c} \right), \quad (58)$$

where:

$$E_2(t) = E_1(t) * h_A(t, L_{ATr12}, R_1, \theta_1) * \delta\left(t - \frac{s_{12}}{c} \right) A_1(s), \quad (59)$$

$$\frac{\partial E_2(t)}{\partial n} = E_1(t) * h_s(t, L_{sTe12}, R_1, \theta_1, s_{12}) * \delta\left(t - \frac{s_{12}}{c} \right) A_1(s). \quad (60)$$

The term $D(L_{S12Re,}, R_2, \theta_2)$ can be transformed into the time domain using the method presented in Section 3B. It can be written in the following form:

$$d(t) \approx \begin{cases} d_{12}(t) + \\ \operatorname{Re}\left\{ \sum_{n=1,3} \overset{+}{d}_{1n}(t) + \overset{+}{d}_{2<}(t) \right\} & \xi \leq 0.35 \\ d_{12}(t) + \\ \operatorname{Re}\left\{ \sum_{n=1,3} \overset{+}{d}_{1n}(t) + \overset{+}{d}_{2>}(t) \right\} & \xi > 0.35 \end{cases}, \quad (61)$$

where:

$$d_{12}(t) = \frac{L^2 \theta^2}{2\pi \sqrt{2ct}\left(t + \frac{X}{c} \right)}, \quad (62)$$

$$\overset{+}{d}_{11}(t) = \frac{1}{\pi} \sqrt{\frac{c}{2\pi}} \frac{L}{e^{j\pi/4}} \left(\frac{-1}{jt} \right)^{1/2} \Gamma\left(\frac{1}{2} \right), \quad (63)$$

$$\overset{+}{d}_{13}(t) = \frac{1}{\pi} \sqrt{\frac{c}{2\pi}} \frac{ce^{j\pi/4}}{\theta^2} \left(\frac{-1}{jt} \right)^{-1/2} \Gamma\left(\frac{-1}{2} \right), \quad (64)$$

$$\overset{+}{d}_{S2>}(t) = \frac{-c}{\pi} \sum_{n=0}^{N} 3\sqrt{\gamma_n \theta} A_n \sum_{m=0}^{M} \frac{j^m}{m!} \Gamma\left(3m + \frac{1}{2} \right) \left[\frac{t}{(\gamma \theta)^3} \right]^m, \quad (65)$$

$$\overset{+}{d}_{2<}(t) \approx \frac{c}{\pi} \sum_{n=0}^{N} n B_n \theta^{n-1} \left(\frac{-1}{jt} \right)^{\frac{n}{3} - \frac{1}{5}} \Gamma\left(\frac{n}{3} - \frac{1}{6} \right) -$$

$$\frac{c}{\pi} \sqrt{\frac{c}{2\pi}} \frac{e^{-j\pi/4}}{\theta^2} \left(\frac{-1}{jt} \right)^{-1/2} \Gamma\left(\frac{-1}{2} \right), \quad (66)$$

Fig. 5 shows the distortion of the incident UWB pulse with the same values of parameters of (42) as in Section 3C. The values of parameters of the convex objects are: θ_1=0.15, θ_2=0.20, R_1=200m, R_2=150m.

6 CONCLUSIONS

The paper presents a new way of deriving the TD-UTD solution for diffraction coefficient of a smooth convex conducting object. The resulting formulas are used to investigate an UWB pulse distorted by a convex diffracting object. The derived TD-UTD solutions involve the same ray paths as the FD-UTD solution from which they were transformed. The authors propose two methods for obtaining the TD-UTD solution: an analytical-numerical method and a purely

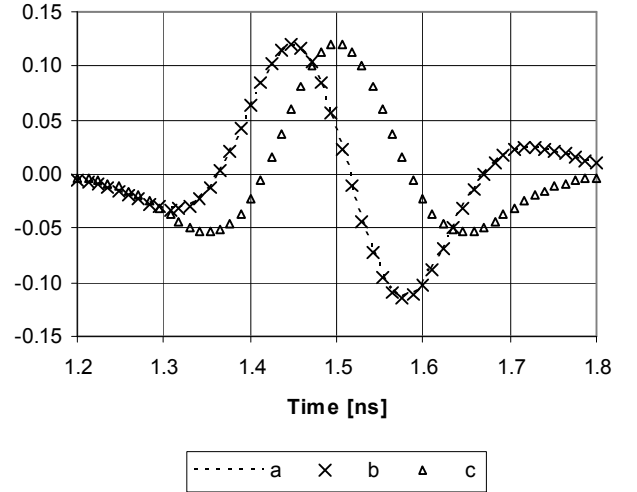**UWB pulse distortion (Amplitude + Slope diffraction)**

Fig. 5. The shape of the distorted UWB pulse with the parameters: a=3ns, t_c=1.ns. Comparison of the results of the pulse distortion obtained trough IFFT (a) with the results of the pulse distortion obtained through direct time domain calculations (b), incident UWB pulse normalized to the amplitude of the distorted pulse (c).

analytical method. Each of them leads to a different TD-UTD formulation for the diffraction coefficient of a convex obstacle. The first formulation obtained through the analytical-

numerical method is related to particular values of convex obstacle parameters and the second one is a formulation of a generalized form, but its application is limited to a given range of values of convex obstacle parameters. However, using the latter formulation for a specified range of parameters of the convex obstacle ensures very good accuracy in determining the pulse distortion. The application of the first formulation gives results which are only slightly worse.

The paper also presents an extension of the TD-UTD solution for a diffraction coefficient of a smooth convex obstacle when slope diffraction is included. Slope diffraction is important when one scattering object or the receiver is in the transition zone of the preceding convex scattering object. We have examined the distortion of a particular UWB pulse caused by two cascaded convex objects (see Fig. 5). Although (41) and (52) relates to soft polarization case alternative formulas can be derived for hard polarization case using similar method to that applied for soft polarization case. Comparing Figures 3 and 5, we may conclude that the pulse distorted by two obstacles resembles the shape of the derivative of an incident pulse, given in (42). It can be seen from Fig.3 that between the incident pulse and the distorted pulse there is a shift in the time domain caused by a convex obstacle. This shift must be taken into account during analysing of problems concerning distance measuring or synchronisation of the received pulses at the receiver. TD-UTD solutions presented in the paper can be used to solve a wider scope of transient problems, where the propagation channels with convex obstacles are investigated, for example when a transmitter and receiver are separated by a row of hills of arbitrary size and height or by a row of buildings with convex-shaped roofs.

7 REFERENCES

[1] M.Z. Win, R.A. Scholtz, Impulse radio: How it works, IEEE Commun. Lett. Vol. 2, pp. 36-38, Feb 1998

[2] D. Porcino, W. Hirt , Ultra-wideband radio technology: potential and challenges ahead, IEEE Commun. Mag., pp. 2-11, July 2003

[3] A. F. Molisch, Ultra-wideband propagation channels – theory, measurement and modeling, IEEE Transactions on Vehicular Technology, vol. 54, no. 5, September 2005, pp. 1528-1545

[4] R. C. Qiu, I. -T. Lu, Wideband wireless multipath channel modeling with path frequency dependence, Conference Record, International Conference on Converging Technologies for Tomorrow's Applications, 23-27 Jun 1996, pp 277 - 281 vol 1.

[5] R. C. Qiu, A Generalized Time Domain Multipath Channel and its Application in Ultra-Wideband (UWB) Wireless Optimal Receiver Design - Part II: Physics Based System Analysis, IEEE Transactions on Wireless Communications, vol. 3, no. 6, November 2004, pp. 2312-2324

[6] R. C. Qiu, A study of the ultra-wideband wireless propagation channel and optimum UWB receiver design, IEEE Journal on Selected Areas in Communications, vol. 20, no. 9, December 2002, pp. 1628-1637

[7] R. C. Qiu, A Generalized Time Domain Multipath Channel and its Application in Ultra-Wideband (UWB) Wireless Optimal Receiver Design - Part III: System Performance Analysis, IEEE Transactions on Wireless Communications, vol. 5, no. 10, October 2006, pp. 2685-2695

[8] R. C. Qiu, Chenming Zhou, Qingchong Liu, Physics-based pulse distortion for ultra-wideband signals, IEEE Transactions on Vehicular Technology, vol. 54, no. 5, September 2005, pp. 1546-1555

[9] J. R. Wait, A. M. Conda., On the diffraction of electromagnetic pulses by curved conducting surfaces, Canadian Journal of Physics, vol. 37, 1959, pp. 1384-1396

[10] D. A. McNamara, C. W. I. Pistorius, Introduction to the uniform geometrical theory of diffraction, Artech House, Boston 1990.

[11] P. H. Pathak, W. Burnside, R. Marhefka, A uniform GTD analysis of the diffraction of electromagnetic waves by a smooth convex surface, IEEE Transactions on Antennas and Propagation, vol. 28, no. 5, September 1980, pp. 631-642.

[12] Chenming Zhou , R. Qiu, Pulse distortion caused by cylinder diffraction and its impact on

UWB communications, The IEEE 2006 International Conference on Ultra-Wideband, Waltham, MA, September 2006, pp.645-650

[13] P. R. Rousseau, P. H. Pathak, Hsi-Tseng Chou, A time domain formulation of the uniform geometrical theory of diffraction for scattering from a smooth convex surface, IEEE Transactions on Antennas and Propagation, vol. 55, no. 6, June 2007, pp. 1522-1534

[14] J. B. Andersen, UTD Multiple-Edge Transition Zone Diffraction, IEEE Transactions on Antennas and Propagation, vol. 45, no. 7, July 1997, pp. 1093-1097

[15] P. R. Rousseau, P. H. Pathak, Time-domain uniform geometrical theory of diffraction for a curved wedge, IEEE Transactions on Antennas and Propagation, vol. 43, no. 12, December 1995, pp 1375-1382.

[16] P. R. Rousseau, P. H. Pathak, TD-UTD slope diffraction for a perfectly conducting curved wedge, Antennas and Propagation Society International Symposium, Newport Beach, 18-23 June 1995, vol. 2, pp. 856-859

[17] G. Koutitas, C. Tzaras, A UTD Solution for Multiple Rounded Surfaces, IEEE Transactions on Antennas and Propagation, vol. 54, no. 4, April 2006, pp 1277-1283.

[18] P.Górniak, W. Bandurski, UWB pulse distortion in the channel containing cylindrical hill, First European Conference on Antennas and Propagation, Nice, 6-10 November, 2006.

[19] P.Górniak, W. Bandurski, Time Domain Version of the Bertoni's Frequency Domain Hill Model, Loughborough Antennas and Propagation Conference, 2-3 April 2007

[20] P.Górniak, W. Bandurski, Time domain model of multiple convex objects transition zone diffraction, Second European Conference on Antennas and Propagation, Edinburgh ,11-16 November, 2007.

[21] H. L. Bertoni, Radio propagation for modern wireless systems, Upper Saddle River, N. Jersey, 2000.

[22] B. Gustavsen, A. Semlyen, Rational approximation of frequency domain response by vector fitting, IEEE Tran. on Power Delivery, vol.14, no. 3, 1999, pp. 1052-1061.

[23] http://www.sintef.no/content/page1____3704. aspx

[24] N. A. Logan, General research in diffraction theory, Lockheed Missiles and Space Division, Tech. Rep. LMSD-288087, 1959.